Electronic Supplementary Information

New AIEgens containing dibenzothiophene-S,S-dioxide and tetraphenylethene moieties: similar structures but much different hole/electron transport properties

Xuejun Zhan,[1,4] Zhongbin Wu,[2,4] Yuxuan Lin,[1] Sheng Tang,[1] Jie Yang,[1] Jie Hu,[1] Qian Peng,[3] Dongge Ma,*[2] and Qianqian Li,[1] Zhen Li*[1]

[1]Department of Chemistry, Hubei Key Lab on Organic and Polymeric Opto-Electronic Materials, Wuhan University, Wuhan, 430072, China.

E-mail: lizhen@whu.edu.cn or lichemlab@163.com

[2] Changchun Institute of Applied Chemistry, Chinese Academy of Sciences, Changchun 130022, China

E-mail: mdg1014@ciac.ac.cn

[3] Institute of Chemistry, The Chinese Academy of Sciences, Beijing, China.

[4]The authors contributed equally to this paper.

Table of Contents

1. **Chart S1.** Several molecules disclosing various approaches to suppress intramolecular charge transfer.
2. **Figure S1.** TGA curves recorded under N_2 at a heating rate of 10 ^{o}C/min.
3. **Figure S2.** DSC curves recorded under N_2 at a heating rate of 10 ^{o}C/min.
4. **Figure S3.** UV spectra in THF solution (10 μM) (A) and in the film state (B).
5. **Figure S4.** PL spectra in the film state.
6. **Figure S5.** (A) PL spectra of **DBTO-*p*TPE** in THF/H_2O mixtures with different water fractions (f_w). Concentration (μM): 10; excitation wavelength (nm): 370. (B) Plots of fluorescence quantum yields determined in THF/H_2O solutions using 9,10-diphenylanthracene (Φ = 90% in cyclohexane) as standard versus water fractions. Inset in (B): photos in THF/water mixtures (f_w = 0 and 99%) taken under the illumination of a 365 nm UV lamp.
7. **Figure S6.** (A) PL spectra of **DBTO-MeTPE** in THF/H_2O mixtures with different water fractions (f_w). Concentration (μM): 10; excitation wavelength (nm): 350. (B) Plots of fluorescence quantum yields determined in THF/H_2O solutions using 9,10-diphenylanthracene (Φ = 90% in cyclohexane) as standard versus water fractions. Inset in (B): photos in THF/water mixtures (f_w = 0 and 99%) taken under the illumination of a 365 nm UV lamp.
8. **Figure S7.** (A) PL spectra of **DBTO-*m*TPE** in THF/H_2O mixtures with different water fractions (f_w). Concentration (μM): 10; excitation wavelength (nm): 320. (B) Plots of fluorescence quantum yields determined in THF/H_2O solutions using 9,10-diphenylanthracene (Φ = 90% in cyclohexane) as standard versus water fractions. Inset in (B): photos in THF/water mixtures (f_w = 0 and 99%) taken under the illumination of a 365 nm UV lamp.
9. **Figure S8.** Calculated molecular orbital amplitude plots of HOMO and LUMO levels and optimized molecular structures.
10. **Figure S9.** (a) Current density-voltage-luminance characteristics, (b) Change in current efficiency with the current density in multilayer EL devices and (c-e) EL spectra of the AIEgens **DBTO-*p*TPE** (device A, c), **DBTO-MeTPE** (device B, d) and **DBTO-*m*TPE** (device C, e) at different voltages. Device configurations: ITO / MoO_3 (10 nm) / NPB (60 nm) / mCP (10 nm) / EML (15 nm) / TPBi (30 nm) / LiF (1.5 nm) /Al.
11. **Figure S10.** (a) Luminance-current density characteristics, (b) Power efficiency- current density characteristics, (c) External quantum efficiency- current density characteristics and (d) Current efficiency-luminance characteristics of the AIEgens **DBTO-*p*TPE** (device A), **DBTO-MeTPE** (device B) and **DBTO-*m*TPE** (device C). Device configurations: ITO / MoO_3 (10 nm) / NPB (60 nm) / mCP (10 nm) / EML (15 nm) / TPBi (30 nm) / LiF (1.5 nm) /Al.

12. **Figure S11.** Energy level diagram of the multilayer devices.
13. **Figure S12-17.** NMR spectra of **DBTO-*p*TPE**, **DBTO-MeTPE** and **DBTO-*m*TPE**.

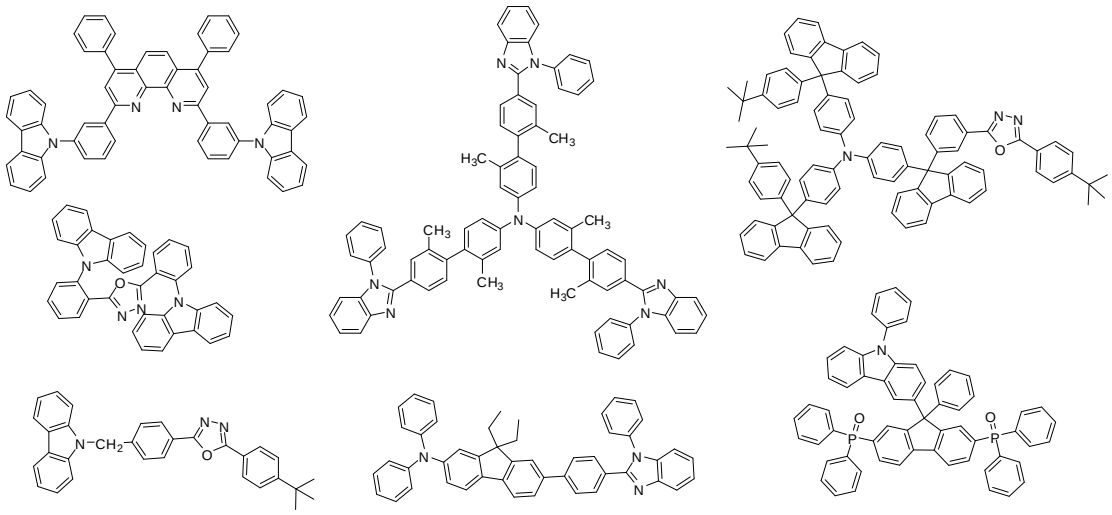

Chart S1. Several molecules disclosing various approaches to suppress intramolecular charge transfer.

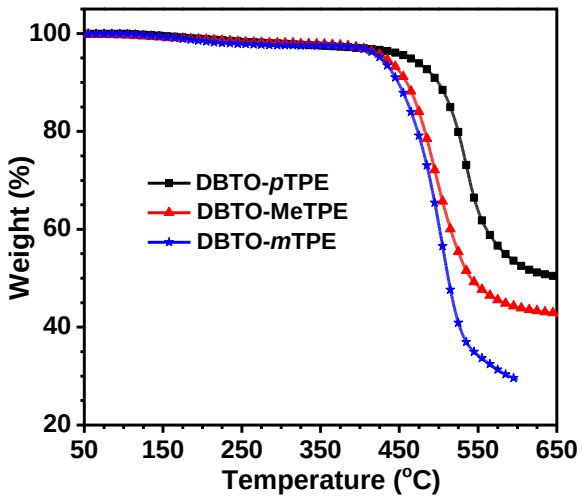

Figure S1. TGA curves recorded under N_2 at a heating rate of 10 ^{o}C/min.

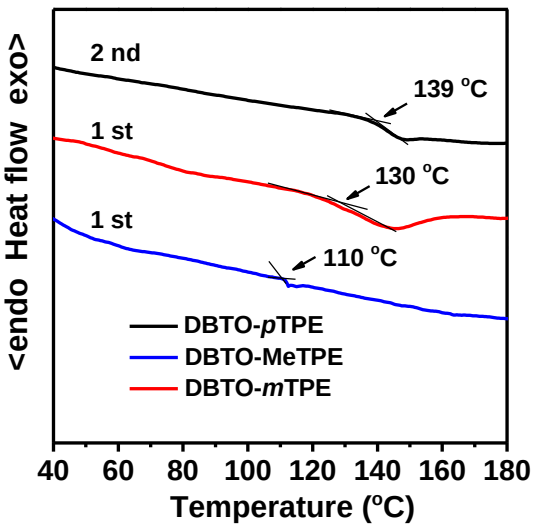

Figure S2. DSC curves recorded under N_2 at a heating rate of 10 ^{o}C/min.

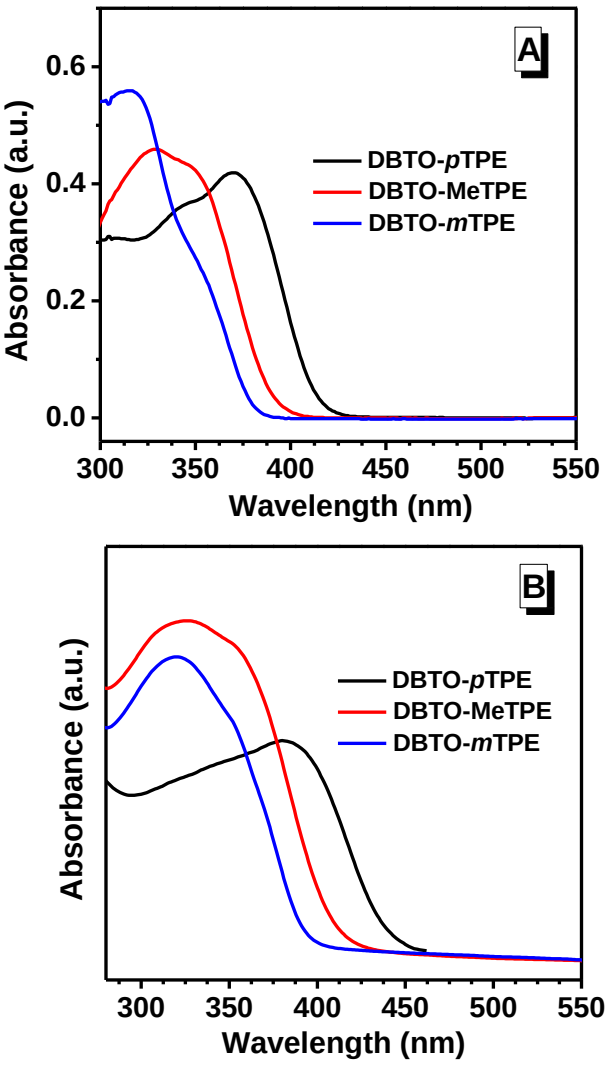

Figure S3. UV-vis spectra in THF solution (~10 μM) (A) and in the thin solid film (B).

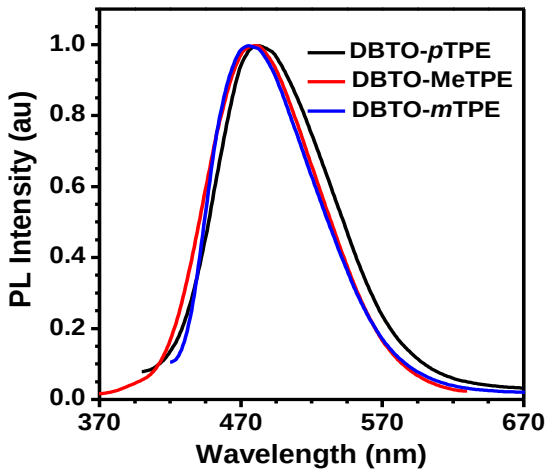

Figure S4. PL spectra in the solid films.

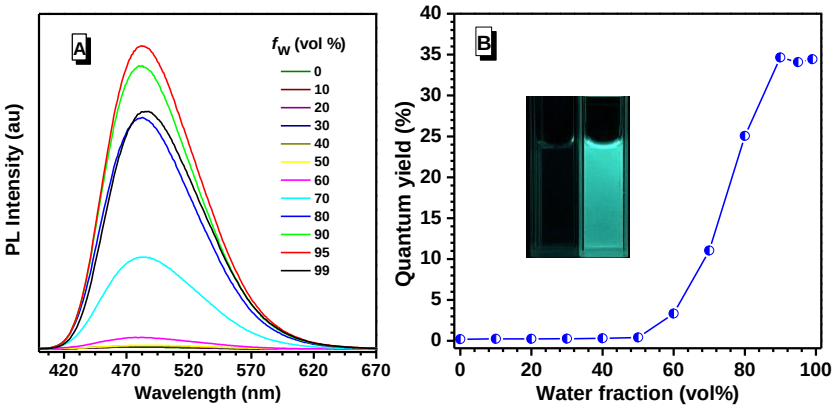

Figure S5. (A) PL spectra of **DBTO-*p*TPE** in THF/H_2O mixtures with different water fractions (f_w). Concentration (μM): 10; excitation wavelength (nm): 370. (B) Plots of fluorescence quantum yields determined in THF/H_2O solutions using 9,10-diphenylanthracene (Φ = 90% in cyclohexane) as standard versus water fractions. Inset in (B): photos of SFTPE in THF/water mixtures (f_w = 0 and 99%) taken under the illumination of a 365 nm UV lamp.

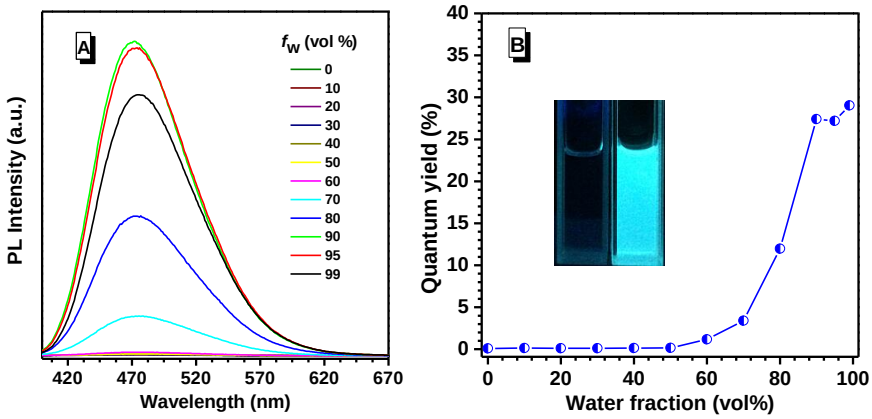

Figure S6. (A) PL spectra of **DBTO-MeTPE** in THF/H_2O mixtures with different water fractions (f_w). Concentration (μM): 10; excitation wavelength (nm): 350. (B) Plots of fluorescence quantum yields determined in THF/H_2O solutions using 9,10-diphenylanthracene (Φ = 90% in cyclohexane) as standard versus water fractions. Inset in (B): photos of SFTPE in THF/water mixtures (f_w = 0 and 99%) taken under the illumination of a 365 nm UV lamp.

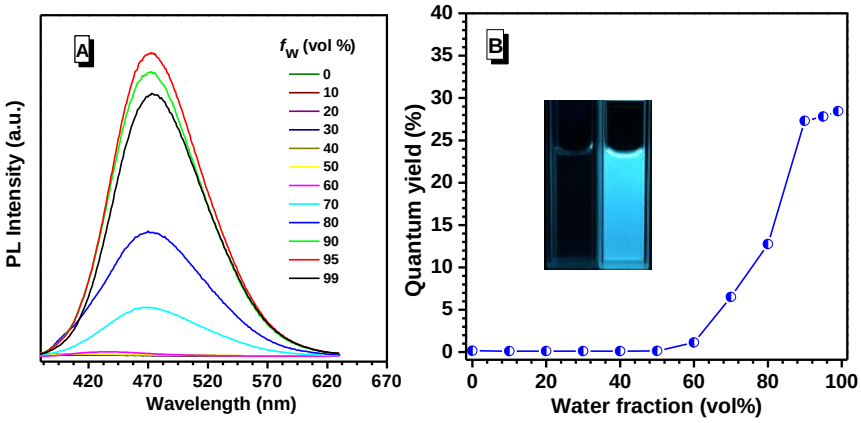

Figure S7. (A) PL spectra of **DBTO-*m*TPE** in THF/H_2O mixtures with different water fractions (f_w). Concentration (μM): 10; excitation wavelength (nm): 320. (B) Plots of fluorescence quantum yields determined in THF/H_2O solutions using 9,10-diphenylanthracene (Φ = 90% in cyclohexane) as standard versus water fractions. Inset in (B): photos of SFTPE in THF/water mixtures (f_w = 0 and 99%) taken under the illumination of a 365 nm UV lamp.

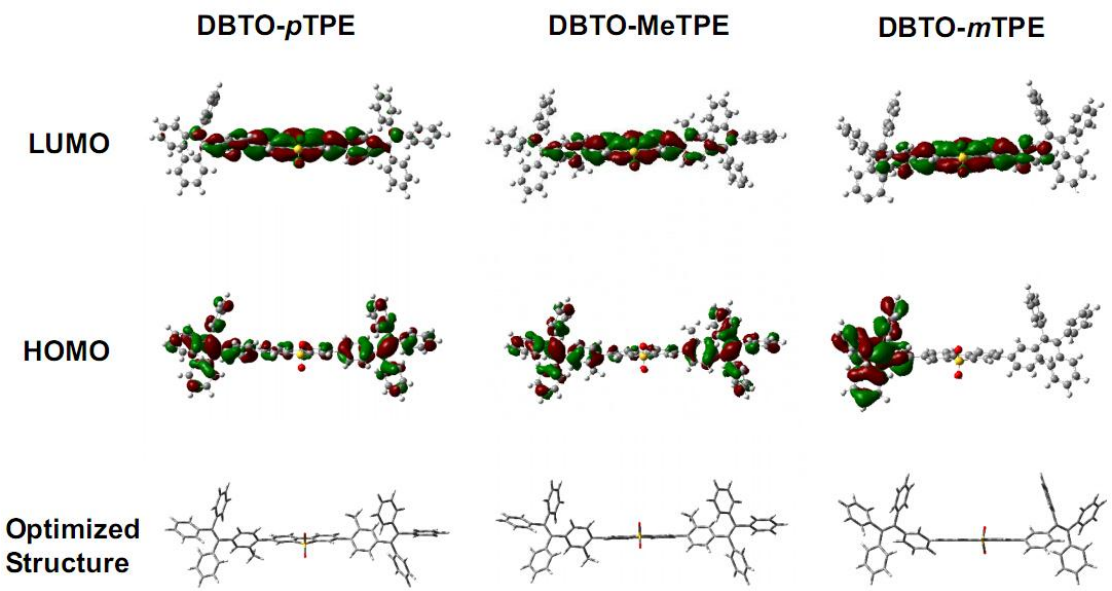

Figure S8. Calculated molecular orbital amplitude plots of HOMO and LUMO levels and optimized molecular structures.

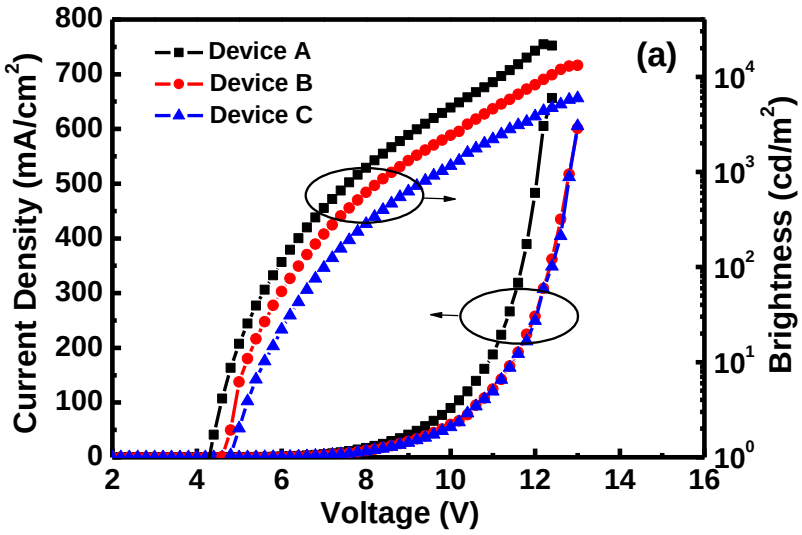
(a)
Device A
Device B
Device C
Current Density (mA/cm^2)
Brightness (cd/m^2)
Voltage (V)
0
100
200
300
400
500
600
700
800
2
4
6
8
10
12
14
16
10^0
10^1
10^2
10^3
10^4

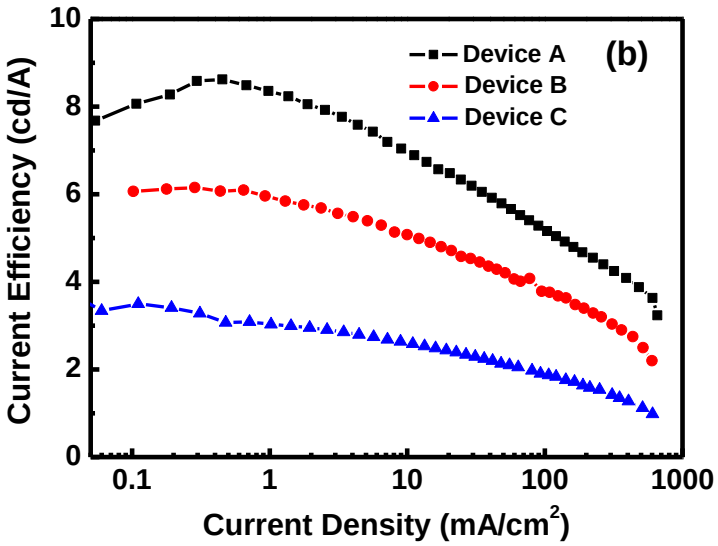
(b)
Device A
Device B
Device C
Current Efficiency (cd/A)
Current Density (mA/cm^2)
0
2
4
6
8
10
0.1
1
10
100
1000

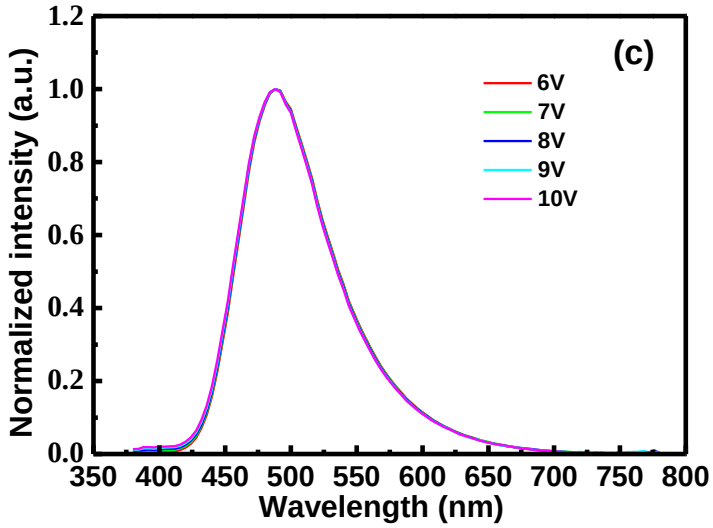
(c)
6V
7V
8V
9V
10V
Normalized intensity (a.u.)
Wavelength (nm)
0.0
0.2
0.4
0.6
0.8
1.0
1.2
350
400
450
500
550
600
650
700
750
800

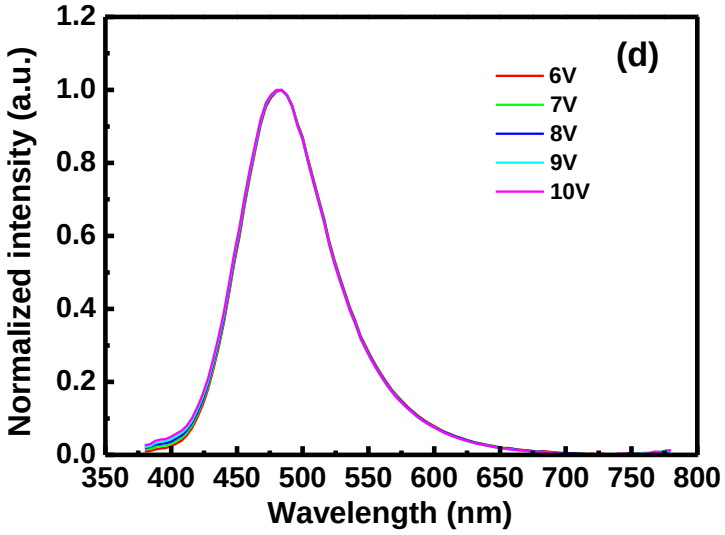
(d)
6V
7V
8V
9V
10V
Normalized intensity (a.u.)
Wavelength (nm)
0.0
0.2
0.4
0.6
0.8
1.0
1.2
350
400
450
500
550
600
650
700
750
800

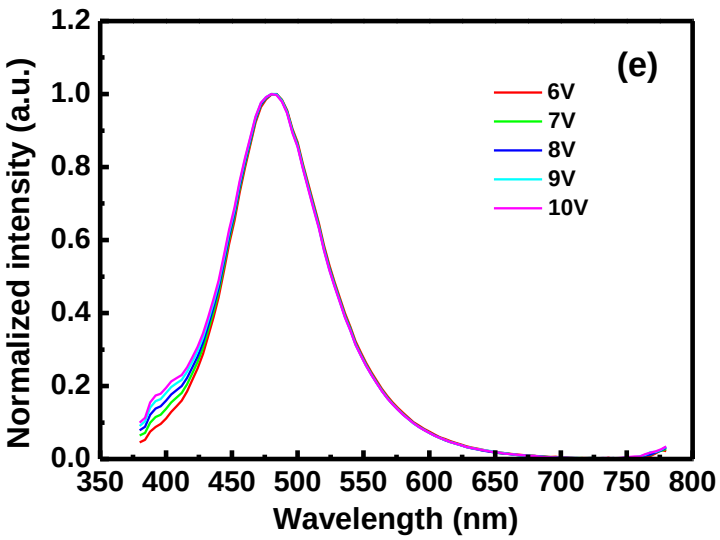

Figure S9. (a) Current density-voltage-luminance characteristics, (b) Change in current efficiency with the current density in multilayer EL devices and (c-e) EL spectra of the AIEgens **DBTO-*p*TPE** (device A, c), **DBTO-MeTPE** (device B, d) and **DBTO-*m*TPE** (device C, e) at different voltages. Device configurations: ITO / MoO_3 (10 nm) / NPB (60 nm) / mCP (10 nm) / EML (15 nm) / TPBi (30 nm) / LiF (1.5 nm) /Al.

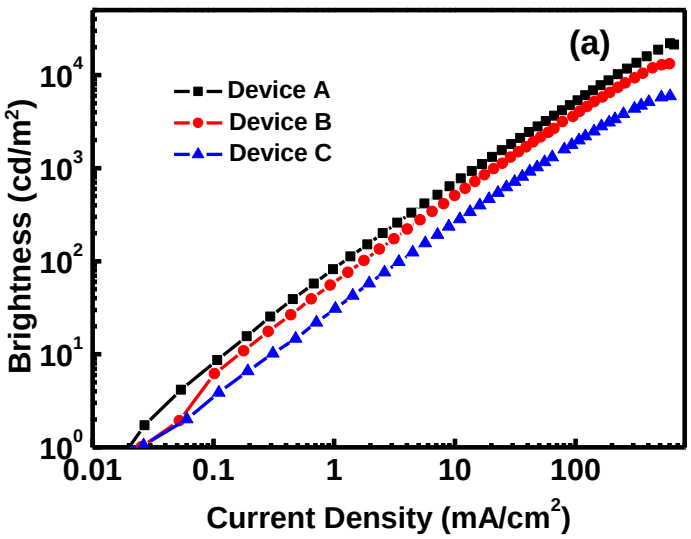

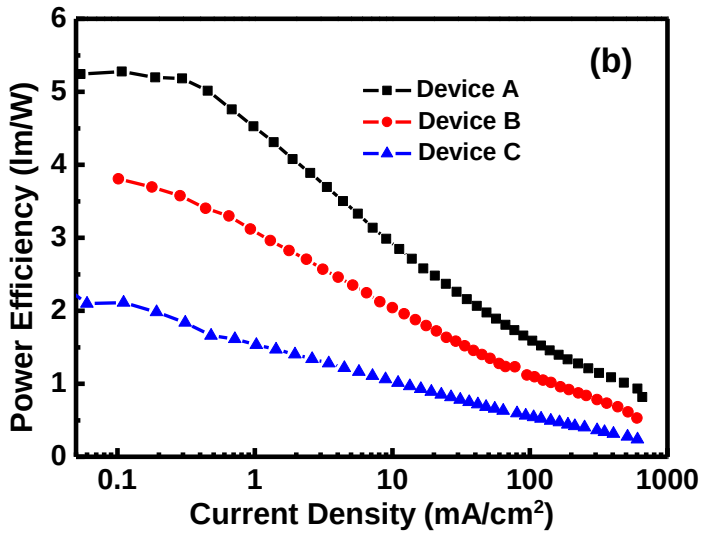
(b)
Device A
Device B
Device C
Power Efficiency (lm/W)
Current Density (mA/cm2)
0
1
2
3
4
5
6
0.1
1
10
100
1000

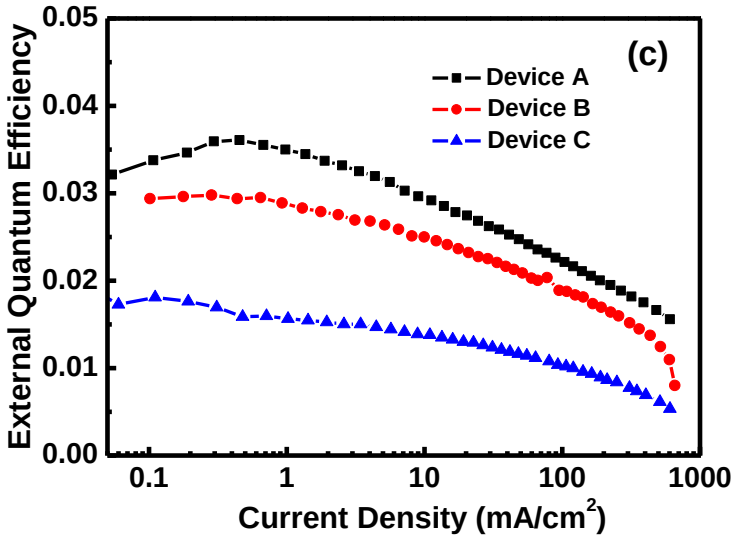
(c)
Device A
Device B
Device C
External Quantum Efficiency
Current Density (mA/cm2)
0.00
0.01
0.02
0.03
0.04
0.05
0.1
1
10
100
1000

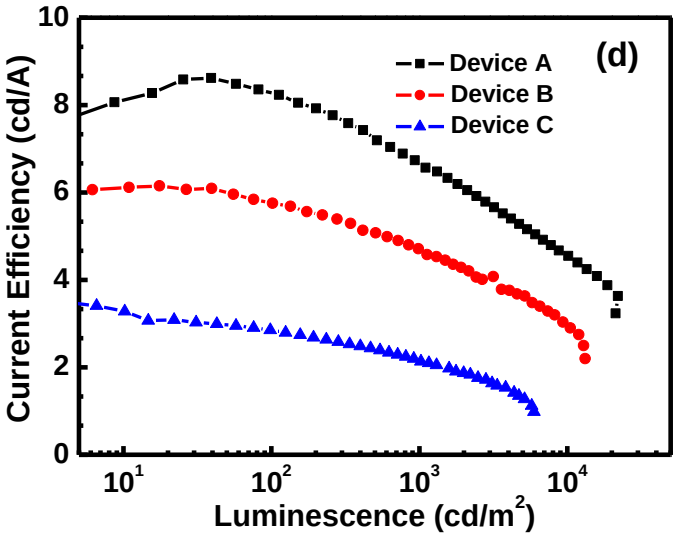

Figure S10. (a) Luminance-current density characteristics, (b) Power efficiency- current density characteristics, (c) External quantum efficiency- current density characteristics and (d) Current efficiency-luminance characteristics of the AIEgens **DBTO-*p*TPE** (device A), **DBTO-MeTPE** (device B) and **DBTO-*m*TPE** (device C). Device configurations: ITO / MoO_3 (10 nm) / NPB (60 nm) / mCP (10 nm) / EML (15 nm) / TPBi (30 nm) / LiF (1.5 nm) /Al.

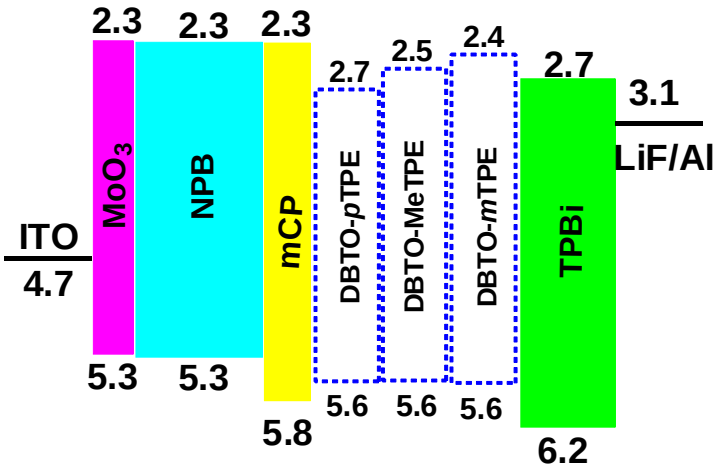

Figure S11. Energy level diagram of the multilayer devices.

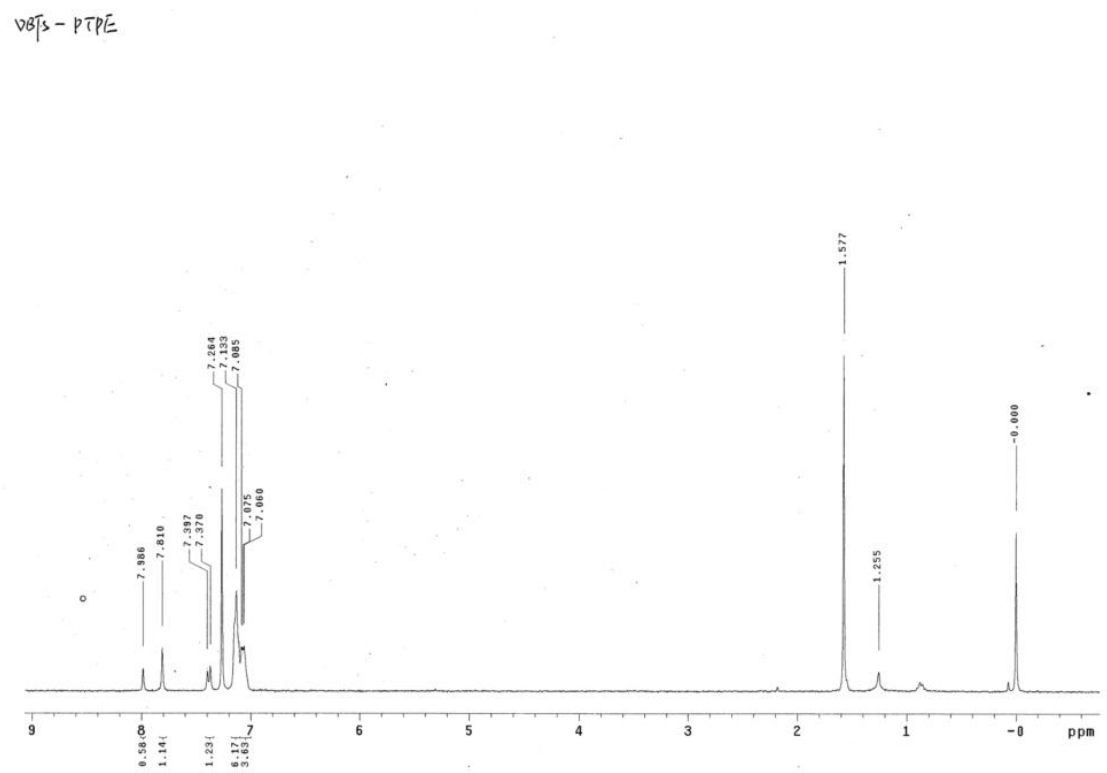

Figure S12. ^{1}H NMR spectrum of the **DBTO-*p*TPE** in $CDCl_3$.

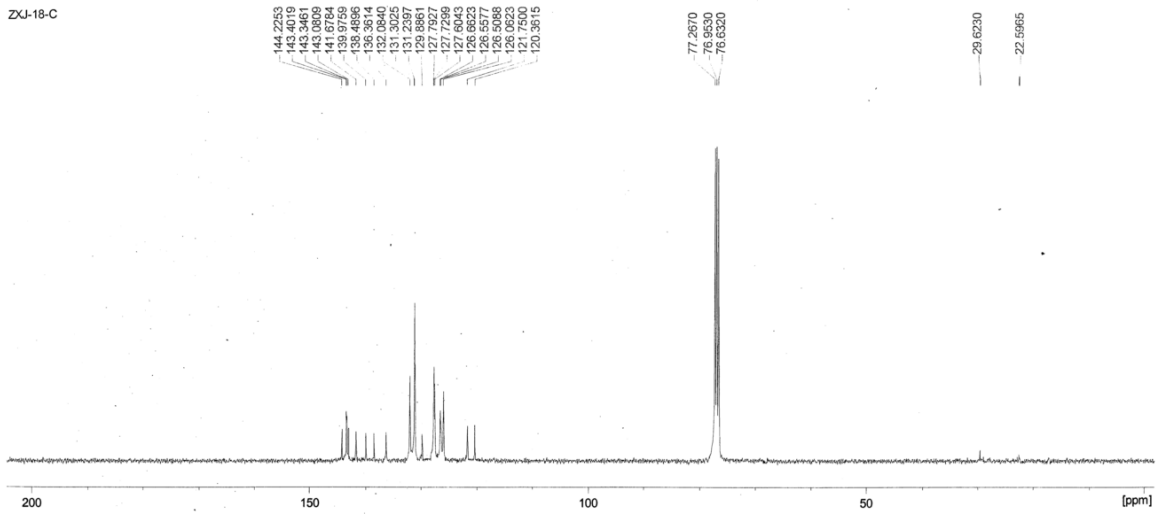

Figure S13. ^{13}C NMR spectrum of the **DBTO-*p*TPE** in $CDCl_3$.

DBTs – MeTPE

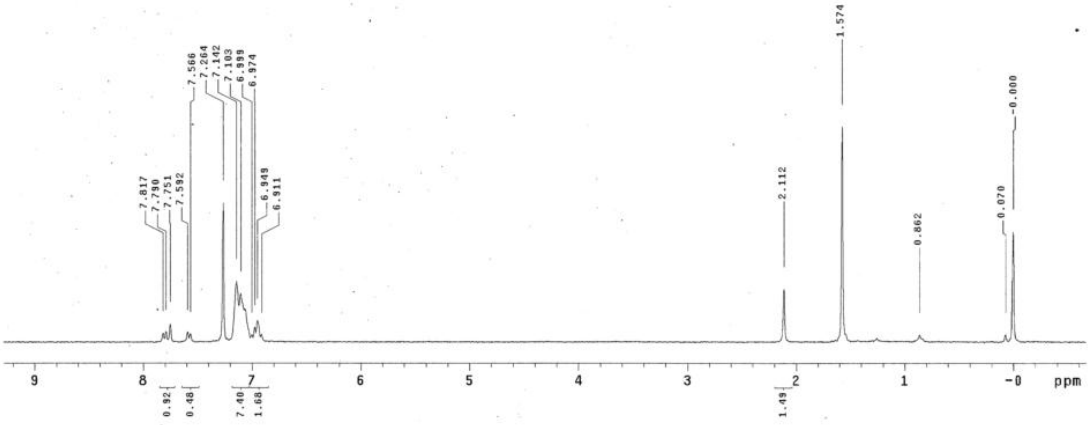

Figure S14. ^{1}H NMR spectrum of the **DBTO-MeTPE** in $CDCl_3$.

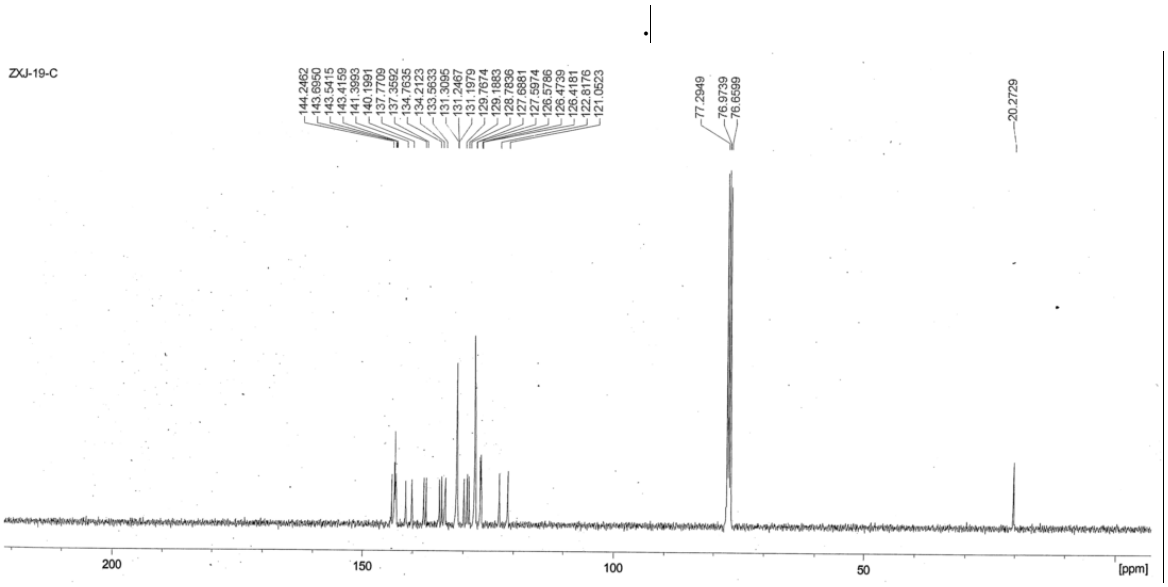

Figure S15. ^{13}C NMR spectrum of the **DBTO-MeTPE** in $CDCl_3$.

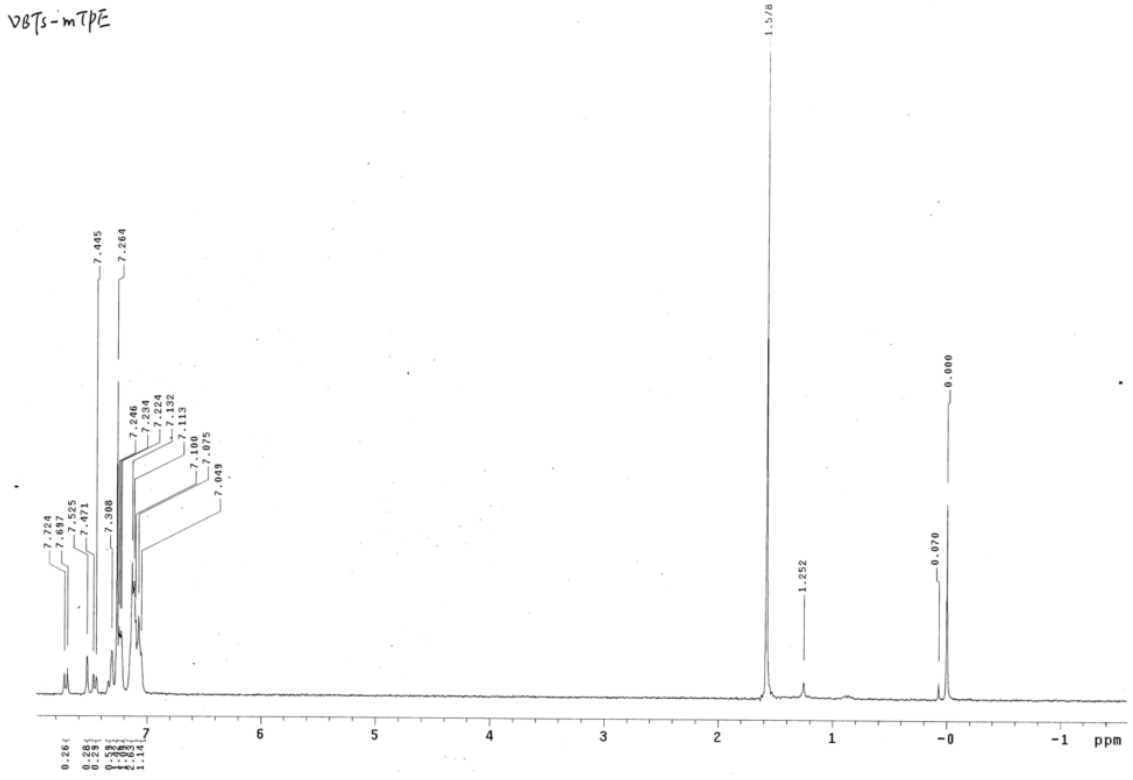

Figure S16. ^{1}H NMR spectrum of the **DBTO-*m*TPE** in $CDCl_3$.

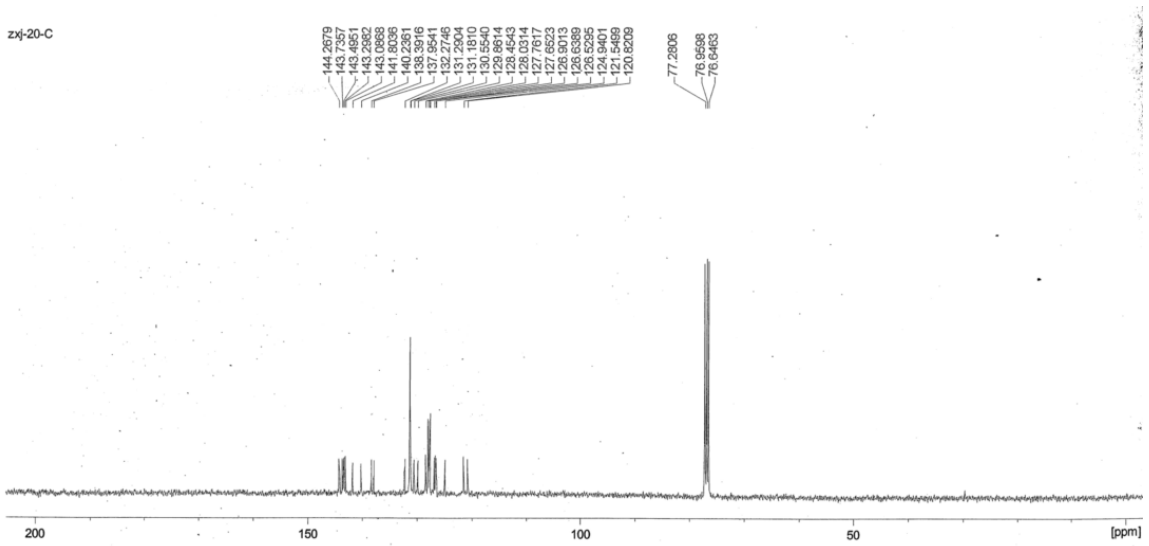

Figure S17. ^{13}C NMR spectrum of the **DBTO-*m*TPE** in $CDCl_3$.